Cell Reports

Supplemental Information

The Nuclear Orphan Receptor NR2F6 Is a Central Checkpoint for Cancer Immune Surveillance

Natascha Hermann-Kleiter, Victoria Klepsch, Stephanie Wallner, Kerstin Siegmund, Sebastian Klepsch, Selma Tuzlak, Andreas Villunger, Sandra Kaminski, Christa Pfeifhofer-Obermair, Thomas Gruber, Dominik Wolf, and Gottfried Baier

Supplemental Experimental Procedures

Mice. *Nr2f6*-deficient mice (Warnecke et al., 2005) back-crossed on C57BL/6 background were used. Wild-type C57BL/6 TRAMP (Tg(TRAMP)8247Ng) mice were crossed into *Nr2f6*-deficient mice to generate *Nr2f6*$^{-/-\text{TRAMP}}$ and *Nr2f6*$^{+/+\text{TRAMP}}$ mice. *Rag*1$^{-/-}$ (B6.129S7-*Rag*1$^{\text{tm1Mom}}$/J) mice were provided by A. Moschen and used for adoptive CD3^{+} cell transfer experiments. Mice were maintained under SPF conditions. All animal experiments have been performed in accordance with national and European guidelines and have been reviewed and authorized by the committee on animal experiments (BMWFW-66.0ll/0128-WF/V/3b/2014) .

Tumor induction and adoptive cell transfer. 1×10^{5} B16-OVA, 3×10^{5} B16-F10 cells, 1.5×10^{5} EG7 cells, or 1×10^{6} TRAMP-C1 cells (purchased from the ATCC, CRL-2730) were injected subcutaneously (s.c.) into the left flank of 8- to 12-week-old mice. Tumor memory experiments were performed via s.c. injection of 1.5×10^{6} EG7 cells into 1 year old *Nr2f6*$^{-/-}$ mice, which rejected primary tumor challenge. Tumor growth was monitored three times per week by measuring tumor length and width. Tumor volume was calculated according to the following equation: ½(length × width^{2}). For survival analysis, mice with tumors greater than the length limit of 15 mm were sacrificed and counted as dead. Adoptive cell transfer (ACT) of *Nr2f6*$^{+/+}$ or *Nr2f6*$^{-/-}$ CD3^{+} T cells into *Rag*1$^{-/-}$ mice was performed 14 days prior tumor induction by injecting 1×10^{7} CD3^{+} T using the Pan T Cell Isolation Kit II mouse (Miltenyi Biotech 130-095-130) via intra-peritoneal injection.

***In vivo* antibody blockade**. Mice were injected s.c. with 5x10^{5} B16-OVA melanoma cells and administered with either 0.5mg of an anti-mouse IFNγ (Clone R4-6A2; BE0054; BioXCell), anti-mouse IL-2 (Clone S4B6-1; BE0043-1), anti-mouse PD-L1 (Clone10F.9G2; BE0101) or corresponding IgG1 (Clone 2A3; BE0089), IgG2b (LTF-2; BE0090) or IgG2a (Clone HRPN; BE0088) control (all from BioXCell, USA) every 3 days starting from day 1 of B16-OVA challenge according to (Zou et al., 2014).

Therapeutic adoptive cell transfer. C57BL/6 wild-type mice at 8 to 12 weeks of age were injected with 1×10^{5} B16-OVA melanoma cells and left untreated until day 7 to establish clearly visible tumors. For adoptive transfers CD3^{+} T cells either from *Nr2f6*$^{+/+}$ or *Nr2f6*$^{-/-}$ tumor antigen naïve mice or *Nr2f6*$^{+/+}$ or *Nr2f6*$^{-/-}$ OT-I transgenic mice were isolated using the

Pan T cell Isolation Kit II (Miltenyi Biotec, 130-095-130) and 1×10^7 $CD3^+$ or 3×10^6 OT-I donor T cells were injected intraperitoneally on day 7 after tumor induction and tumor growth was subsequently measured as described above.

Preparation of tumor infiltrating cells. Mononuclear infiltrating cells were isolated from both subcutaneous and autochthonous tumors at the indicated time points. Briefly, tumor tissues from sacrificed mice were prepared by mechanical disruption followed by digestion for 45 min with collagenase D (2.5 mg/ml; Roche, 11088858001) and DNase I (1 mg/ml; Roche, 11284932001) at 37°C. Digested tissues were incubated 5 min at 37°C with EDTA (0.5 M) to prevent DC/T cell aggregates and mashed through a 100-µm filter and a 40-µm filter. Cells were washed, and resuspended in either PBS+2% FCS or IMDM complete medium (10% FCS, 2 mM L-glutamine, and 50 U/ml penicillin/streptomycin).

***Ex vivo* $CD8^+$ T cell analysis**. $CD8^+$ T cells were isolated using either the mouse CD8 T Cell Isolation Kit II (Miltenyi Biotec, 130-090-859) or the human $CD8^+$ T Cell Isolation Kit (Miltenyi Biotec, 130-096-495). Activation of $CD8^+$ T cells was performed in complete IMDM medium in the presence of plate-bound 2C11 (made in house) for mouse or OKT3 for human anti-CD3 (5 µg/ml, eBiosciences, 16-0037) and soluble mouse or human anti-CD28 (1 µg/ml, BD, 553294). Cells were harvested at the indicated time points. For survival and apoptosis assays, spleens and lymph nodes were isolated from *Nr2f6*$^{+/+}$ and *Nr2f6*$^{-/-}$ mice. Single cell suspensions were pooled and stained with fluorochrome-labelled antibodies recognizing mouse CD4 (GK1.5) or mouse CD8a (53-6.7, both from BioLegend), respectively. To exclude dead cells, 12.5µg/mL DAPI was added. Cells were sorted on a BD FacsAria^{TM}III Cell sorter (BD Biosciences). Sorted T cells were cultured at a concentration of $1x10^6$/mL in Roswell Park Memorial Institute (RPMI) 1640 medium (PAA; E15-039), supplemented with 10% FCS, 2 mM L-Glutamine, 1% Penicillin plus Streptomycin (10.000 U/mL Penicillin and 10 mg/mL Streptomycin in 0.9% NaCl), 5×10^{-5} M 2-mercaptoethanol, 50µg/mL Gentamicin, 100µM non-essential amino acids (Gibco, 1091607) and 1 mM sodium pyruvate (Gibco, 1046485). Apoptosis was assessed after 48 hours in culture using Annexin V Apoptosis Detection Kit eFluor® 450 (eBioscience).

Chromatin immunoprecipitation. ChIP assay was performed with a ChIP assay kit according to the recommendations of the manufacturer (Imgenex) in combination with the Cold Spring Harbor protocol (Carey et al., 2009) and previously described methods (Hermann-Kleiter et al., 2012). Briefly, *Nr2f6*$^{+/+}$ and *Nr2f6*-deficient $CD3^+$ T cells were isolated

untouched using the Pan T Cell Isolation Kit II mouse (Miltenyi Biotech, 130-090-861). $CD8^+$ T cells were isolated using either the mouse CD8 T Cell Isolation Kit II (Miltenyi Biotec, 130-104-075) or the human $CD8^+$ T Cell Isolation Kit (Miltenyi Biotec, 130-096-495). T cells were activated using plate-bound anti-CD3 (5µg/ml) and soluble anti-CD28 (1µg/ml) in complete IMDM medium. After activation, cells were harvested at the indicated time points and washed once in IMDM for subsequent fixation in 1% formaldehyde at 37°C for 10 min, and quenching of cross-linking by the addition of 1.375 M glycine. The cells were then washed twice with ice-cold PBS and lysed in cold cell lysis buffer for ChIP [5 mM PIPES (pH 8.0), 85 mM KCl, 0.5% Nonidet P-40 (NP-40)] for 10 min. After centrifugation, the cell pellets were lysed in 1 ml nuclei lysis buffer for ChIP [50 mM Tris-Cl (pH 8.0), 10 mM EDTA, 1% SDS] supplemented with protease inhibitors and incubated for 10 min on ice. After sonication with 25 30-s pulses using a Bioruptor Next Generation (Diagenode), the samples were centrifuged for 10 min at 12,000 rpm. The sheared chromatin was used to set up immunoprecipitation reactions with 5µg of the indicated antibodies (IgG, Santa Cruz sc-2027; NR2F6, R&D PP-N2025-00) at 4°C overnight. Magna ChIP protein G magnetic beads were added for 2h, and the samples were sequentially washed once with the buffers provided by the supplier (Imgenex; high to low salt). The DNA-protein complex was eluted by heating at 65°C overnight, and the DNA was eluted using the IPure kit (Diagenode). Real-time PCR was performed using an ABI PRIM 7000 Sequence Detection System (Applied Biosystems) with the following primers and probes: *Il2* minimal promoter (-380 – ATG): Forward: 5´ TTGTATGAATTAAAACTGCCACCTAAG 3´; Reverse: 5´CACTGACTGAATGGATTTAGGTGAA3´ with the probe 5´FAM-TTGGGCT AACCCGACCAAGAGGGA BHQ1-3 ´(Balasubramani et al., 2010). Distal *Il2* promoter (-1624): Forward: 5´ CAGTGTGCATGTAGCAGTCAA 3´; Reverse: 5´CACCACA CACCTACCCCATTT 3´; *Ifng* minimal promoter (-185): Forward: 5´ CGAGGAGCC TTCGATC AGGT 3´; Reverse: 5´GGTCAGCCGATGGCAGCTA 3´; with the probe 5´FAM TAAAACTGGAAGCCAGAGAGGTGCAGG- BHQ1-3´ (Balasubramani et al., 2010).

Flow cytometry. Splenocytes and lymph node cells were depleted of erythrocytes using the mouse erythrocyte lysing kit (R&D, WL2000) and mashed through a 100-µm filter. Splenocytes, lymph node cells, and TILs were incubated with FcR Block (BD Biosciences, 553142) to prevent nonspecific antibody binding before staining with appropriate surface antibodies for 30 min at 4°C, washed with PBS+2% FCS, and used for FACS analysis. For intracellular cytokine staining, cells were stimulated with 50 ng/ml Phorbol 12,13-dibutyrate (PDBu, Sigma, P1269), 500 ng ionomycin (Sigma, I0634) and GolgiPlug (BD Biosciences,

555029) for 4–5h. After fixation (cytokines: Biolegend fixation buffer (420801), 20 minutes, 4°C; transcription factors: FoxP3 staining buffer set (eBiosciences, 00-5523), >30 minutes, 4°C), cells were permeabilized with the fixation/permeabilization kit (BioLegend, 421002) for cytokines and the Foxp3-staining buffer set (eBiosciences, 00-5523) for transcription factors, incubated with FcR Block (BD Biosciences, 553142) before staining with specific cell surface or intracellular marker antibodies. Data acquisition was performed on a FACSCalibur or LSR Fortessa cell analyzer (Becton Dickinson). Data analysis was conducted using the Flowlogic software (eBioscience, version 1.6.0_35). The following antibodies were used for flow cytometry: CD4-V500 (BD, 560783), CD4-PE (BD, 553049), CD8a-APC (BD, 553035), CD25-PE (BD, 553866), CD11c-PE-Cy7 (BD, 558079), CD44-FITC (BD, 553270), CD62L-APC (BD, 553152), PD-1-PE (BD, 561788), Ki67-PE (BD, 556027), IL-17-PE (BD, 559502), IL-2-APC (BD, 554429), CD45-V500 (BD, 561487), CD11b-PE (BD, 557397), TNFa-PerCP Cy5.5 (BD, 560659), CD45-FITC (eBiosciences, 11-0451-82), CD8a-PerCP Cy5.5 (eBiosciences, 45-0081-82), DX-5-PE-Cy7 (eBiosciences, 25-5971-81), CD44-PerCP Cy5.5 (eBiosciences, 45-0441-82), TCR γδ-APC (eBiosciences, 17-5711-82), Foxp3-PE (eBiosciences, 12-4771-82), RORc (t)-APC (eBiosciences, 17-6988-82), GrzB-PerCP-710 (eBiosciences, 46-8898-82), IFNγ-PE-Cy7 (eBiosciences, 25-7311-82), MHCII-FITC (eBiosciences, 11-5321-82), Ly-6C-APC (eBiosciences, 17-5932-82), PDL-1-PerCP-eFluor710 (eBiosciences, 46-5982-80), CD45-APC (eBiosciences, 17-0451-81), CD3-PE-Cy7 (eBiosciences, 25-0031,82), FoxP3-FITC (eBiosciences, 11-5773-82), CD3-PE (eBiosciences, 12-0031-83), CD8a-bv421 (BioLegend, 100738), F4/80-PE-Cy7 (BioLegend, 123113), CD25-bv421 (BioLegend, 102034), Gr-1-FITC (BioLegend, 108405), F4/80-PE (BioLegend, 123109), CD11b-APC (BioLegend, 101211), Tbet-bv605 (BioLegend, 644817).

Gene expression analysis and MLPA. Total RNA was isolated using the RNeasy® Mini Kit (Quiagen). First-strand cDNA synthesis was performed using oligo(dT) primers (Promega) with the Qiagen Omniscript RT kit, according to the instructions of the supplier and as described previously (Hermann-Kleiter et al., 2012). Expression analysis was performed using real-time PCR with an ABI PRIM 7000 or ABI PRIM 7500fast Sequence Detection System with TaqMan gene expression assays (Applied Biosystems); all expression patterns were normalized to *Gapdh*. Multiplex Ligation-dependent Probe Amplification (MLPA) was performed using the SALSA® MLPA® EK1-RT kit purchased from MRC-Holland and used according to the manufacturer's instructions. Briefly, RNA was isolated, using the Quick-RNA™ MicroPrep (Zymo Research, #R1051) according to the manufacturer's instructions. Specific mRNAs were reversely transcribed into cDNA and bound by two oligonucleotides

consequently ligated by a heat stable ligase forming one probe. Each probe gives rise to an amplification product of unique length, separated by capillary sequencer (Genescan). Analysis was performed with GeneMapper (Applied Biosystems GmbH). The sum of all peak data was set to 100% to normalize for fluctuations between different samples, and single peaks were calculated relative to 100%. The following list of cell death related genes was quantified: BOK, SERPINB9, BCLW, BCLXL, FLIP, GUSB, BCL2, A1, MCL1, BAX, BAK, BCLG, BCLRAMBO, BID, BAD, BIK, BIM, BMF, BID3, MOAP1, APAF1, AIF, BCL2L10, XIAP, SURVIVIN, BIRC1A, BIRC7, CIAP1, CIAP2, NOXA, PUMA, BIRC6, OMI, B2M, TBP, P21, GZMB, PRF1, DIABLO, PAK2.

Treg and iTreg suppression assay. $CD25^+CD4^+$ and $CD25^-CD4^+$ T cells were isolated from spleens and LNs of *Nr2f6*$^{+/+}$ and *Nr2f6*$^{-/-}$ using the $CD4^+$ T cell isolation kit II followed by CD25-PE and anti-PE MicroBeads (all Miltenyi Biotec, 130-048-801) according to the manufacturer's recommendation. Sorted $CD25^-CD4^+$ T cells were labelled with 2.5µM CFSE (Molecular probes, C1157) for 4 min at 37°C; labelling was stopped by addition of fetal calf serum. T cell depleted splenocytes (using CD4 [130-049-201] and CD8a [130-049-401] MicroBeads, Miltenyi Biotec) treated for 45 min with 50µg/ml mitomycin C (AppliChem, A2190,0002) were used - after extensive washing - as APCs. To induce proliferation 0.5µg/ml antiCD3 (145-2C11, BioLegend) was added. $1x10^5$ CFSE-labeled $CD25^-CD4^+$ responder T cells were cultured with $1x10^5$ APCs in 96-well U-bottom tissue culture plates (Falcon). $CD25^+CD4^+$ T cells were added at the ratios 1+1, 1+4 and 1+9. To address suppression by iTregs *in vitro* differentiated iTregs were harvested at day 5 of culture (see below) and dead cells were removed using a dead cell removal kit (Miltenyi Biotec, 120-000-437) according to the manufacturer's recommendation. At day 3 of co-culture proliferation and activation (anti-CD25 staining) was analyzed by flow cytometry; 7-AAD or propidium iodide was added to exclude dead cells.

$CD4^+$ T cell differentiation cultures. Naïve $CD4^+$ T cells were isolated using the $CD4^+CD62L^+$ naïve T cell isolation kit II (Miltenyi Biotech, 130-093-227). Polarization of naïve $CD4^+$ T cells into iTregs was performed with 4µg/ml plate-bound anti-CD3 (clone: 2C11) and 1µg/ml anti-CD28 soluble in the presence of 5ng/ml recombinant mouse TGF-b and recombinant 20ng/ml hIL-2. Th1 polarization was performed with 5µg/ml anti-CD3 and 1µg/ml anti-CD28 in the presence of 10ng/ml mIL-12 and 5µg/ml anti-IL-4 (eBiosciences).

Gel mobility-shift assay. Electromobility assay was performed as described previously (Hermann-Kleiter et al., 2008).

Immunohistochemistry. Cryosections (5-7µm thickness) of TRAMP prostate or B16-OVA tumors from *Nr2f6*$^{+/+}$ and *Nr2f6*$^{-/-}$ mice were fixed and incubated with mouse monoclonal antibodies against the T cell markers CD4 and CD8 overnight at 4°C. Mouse monoclonal antibody anti-human CD4 (M731029, clone 4B12) and mouse monoclonal antibody anti-human CD8, (IS62330, clone C8/144B) were purchased from Dako. IHC analysis of TRAMP prostate and B16-OVA tumors were performed in triplicates of 4 biopsy specimens of *Nr2f6*$^{+/+}$ and *Nr2f6*$^{-/-}$ tumors. The sections were subsequently incubated with anti-mouse IgG Alexa Fluor 488® conjugate and Hoechst for 45 minutes at room temperature and mounted with Dako fluorescent mounting medium (S3023). Digital IHC images were acquired with an Axiovert 40 CFL (ZEISS) microscope.

Analysis of TCRVβ repertoire. Total RNA was prepared from *Nr2f6*$^{+/+}$ or *Nr2f6*$^{-/-}$ naïve or tumor draining inguinal lymph nodes as described in gene expression analysis. For TCRVβ analysis the TCRexpress™ Mouse Repertoire Clonality Detection Kit (BioMed Immunotech, M0561) was used in order to identify the Vβ gene families (from Vβ 1 to 20 with subfamilies Vβ 8.1, 8.2 and 8.3) of the CDR3 region according to the instructions of the supplier.

Statistics. Data were analyzed using Prism 5.03 software (GraphPad Software). Experiments were repeated at least two or three times. Data are represented as indicated (either the mean ± SEM or ± SD) for all figure panels in which error bars are shown. The P values were assessed using two-tailed unpaired student's t-test, log rank test, or ANOVA. A P value of less than 0.05 was considered statistically significant. *$p<0.05$; **$p<0.01$; ***$p<0.001$.

Supplemental References

Balasubramani, A., Shibata, Y., Crawford, G.E., Baldwin, A.S., Hatton, R.D., and Weaver, C.T. (2010). Modular utilization of distal cis-regulatory elements controls Ifng gene expression in T cells activated by distinct stimuli. Immunity 33, 35-47.

Carey, M.F., Peterson, C.L., and Smale, S.T. (2009). Chromatin immunoprecipitation (ChIP). Cold Spring Harbor protocols 2009, pdb prot5279.

Supplemental Figures and legends

Figure S1 related to Figure 1: Characterization of *Nr2f6*$^{+/+TRAMP}$ and *Nr2f6*$^{-/-TRAMP}$ TRAMP tumors and draining lymph nodes at week 22, 28 and endpoint.

Loss of NR2F6 in male TRAMP mice did not change the body weight of *Nr2f6*$^{+/+TRAMP}$ versus *Nr2f6*$^{-/-TRAMP}$ mice (A) at week 22, *Nr2f6*$^{+/+TRAMP}$ (n=9), *Nr2f6*$^{-/-TRAMP}$ (n=5), (B) at week 28, *Nr2f6*$^{+/+TRAMP}$ (n=19), *Nr2f6*$^{-/-TRAMP}$ (n=15) or at (C) endpoint analysis *Nr2f6*$^{+/+TRAMP}$ (n=4), *Nr2f6*$^{-/-TRAMP}$ (n=4). (D) *Nr2f6*-deficiency in male TRAMP mice correlates with higher numbers of TILs and T lymphocytes in dLN at week 28. Dot blots of CD45$^+$CD4$^+$ cells within the tumor dLN of *Nr2f6*$^{+/+TRAMP}$ and *Nr2f6*$^{-/-TRAMP}$ mice. Numbers adjacent to outlined areas indicate the percentage of positive cells relative to parental gate (CD45$^+$). (E) Bar charts depict percentages of CD4$^+$ cells (p=0.012), CD4$^+$CD44$^+$ cells (p=0.009), CD4$^+$INFγ^+ cells (p=0.006) within prostate tumor-draining lymph nodes of *Nr2f6*$^{+/+TRAMP}$ (n=7) and *Nr2f6*$^{-/-TRAMP}$ (n=11) mice are shown. (F) Dot blots of CD45$^+$CD8$^+$ cells within the tumor dLN of *Nr2f6*$^{+/+TRAMP}$ and *Nr2f6*$^{-/-TRAMP}$ mice. Numbers adjacent to outlined areas indicate the percentage of positive cells relative to parental gate (CD45$^+$). (G) Bar charts of total cell percentages within prostate tumor-draining lymph nodes, CD8$^+$ cells (p=0.004), CD8$^+$CD44$^+$ cells (p=0.017), and CD8$^+$INFγ^+ cells (p=0.03) of *Nr2f6*$^{+/+TRAMP}$ (n=7) and *Nr2f6*$^{-/-TRAMP}$ (n=11) mice are shown. (H) Percentages of CD45$^+$CD4$^+$RORc$^+$ as well as CD45$^+$TCR$\gamma\delta^+$ tumor infiltrating cells in *Nr2f6*$^{+/+TRAMP}$ (n=11), *Nr2f6*$^{-/-TRAMP}$ (n=7) mice were increased at week 28, which however did not reach statistical significance. (I) In prostate tumor dLN a tendency towards more CD45$^+$ CD4$^+$IL-17$^+$, CD8$^+$T-bet$^+$, DX5$^+$, and TCR$\gamma\delta^+$ cells could be detected in *Nr2f6*$^{-/-TRAMP}$ (n=7) when compared to *Nr2f6*$^{+/+TRAMP}$ (n=11) mice. (J) Loss of NR2F6 in male TRAMP mice correlates with higher numbers of TILs and cytokine secreting T lymphocytes in dLN at week 22. Gross examination of UG tracts at week 22 from *Nr2f6*$^{+/+TRAMP}$ (n=9) and *Nr2f6*$^{-/-TRAMP}$ (n=5) mice shows decreased UG tract size in *Nr2f6*$^{-/-TRAMP}$ mice. (K) Prostate weight (p=0.003) as well as the ratio between UG tract and body weight (p=0.002) was significantly decreased in *Nr2f6*$^{-/-TRAMP}$ mice. (L) Higher numbers of CD45$^+$ tumor infiltrating lymphocytes (p=0.006) as well as (M) tumor draining lymph node cells, especially CD4$^+$IL-2$^+$ T cells (p=0.007) could be detected in *Nr2f6*$^{-/-TRAMP}$ (n=5) mice when compared to cells isolated from *Nr2f6*$^{+/+TRAMP}$ (n=9) mice, bar charts and representative dot blots are shown. Numbers adjacent to outlined areas indicate percentages of cells within the gates. Results shown are derived from at least two independent experiments. Error bars represent the mean ± SEM.

Figure S2 related to Figure 2: TCRVβ repertoire in naïve and B16-OVA tumor draining lymph nodes of *Nr2f6*$^{+/+}$ and *Nr2f6*$^{-/-}$ mice is not altered.

TCRVβ repertoire of (A) wild-type and (B) *Nr2f6*-deficient T lymphocytes within naive or tumor draining lymph (dLN) nodes was investigated via clonality analysis of the 22 individual Vβ gene families (from Vβ 1 to 20 with subfamilies Vβ 8.1, 8.2 and 8.3) of the CDR3 region. Nested PCR products were separated on a high resolution agarose gel. Data shown are representatives of two independent experiments as well as negative (-) & positive controls (+) are given.

Figure S3 related to Figure 3: Increased numbers of tumor infiltrating T cells in *Nr2f6*-deficient mice bearing B16-OVA transplantable melanomas.

(A) Representative dot plots of tumor infiltrating $CD8^+$ and $CD4^+$ cells gated on $CD45^+$ derived from *Nr2f6*$^{+/+}$ and *Nr2f6*$^{-/-}$ mice. (B) A representative analysis of the flow cytometric gating strategy for discerning tumor infiltrating immune cells is depicted, whereby gated populations (from left to right) are indicated defining forward and side scatter, doublets, $CD45^+CD3^+CD4^+CD8^+$ and as one further example $CD45^+CD3^+CD8^+PD\text{-}1^+$ populations. (C) Tumor immune cell infiltration rate is not dependent on tumor size but differs in general, $CD45^+$ and $CD3^+$ parental cell percentages in small [up to 0.021g; maximum 52.5mm^3], medium [0.022g – 0.111g; maximum 271mm^3] and large [0.112g – 0.370g; maximum 845mm^3] tumors of *Nr2f6*$^{+/+}$ or *Nr2f6*$^{-/-}$ mice are shown by dot blots. (D) Representative cryosections of B16-OVA melanomas from *Nr2f6*$^{+/+}$ or *Nr2f6*$^{-/-}$ mice stained for the T cell markers CD4 and CD8 in green and Hoechst nuclear stain in blue. Scale bar=50µm. (E) Graphical representation of enhanced $CD4^+$ ($p=0.003$), and $CD8^+$ ($p=0.003$) tumor T cell infiltration in *Nr2f6*$^{-/-}$ mice, averaged from three fields per mouse and four mice per genotype. (F) Immune cell numbers and characterization of *Nr2f6*$^{+/+}$ (n=6) and *Nr2f6*$^{-/-}$ (n=7) B16-OVA tumor infiltrating cells analyzed by the following markers and gates: $CD45^+$ ($p=0.0003$), $CD45^+CD3^+$ ($p=0.0002$), $CD45^+CD8^+$ ($p=0.01$), and $CD45^+CD4^+$ ($p=0.005$), as also shown by dot blots in Figure S3A. Error bars represent ± SEM, differences were analyzed using student's t-test.

Figure S4 related to Figure 4: *Nr2f6* expression impairs expression of IL-2 and IFNγ as well as activation markers within the tumor draining lymph nodes.

Analysis of B16-OVA tumor-draining lymph nodes from *Nr2f6*$^{+/+}$ and *Nr2f6*$^{-/-}$ mice on day 14 are shown. (A) Dot blots of enhanced CD45^{+}CD4^{+} cell numbers in *Nr2f6*$^{-/-}$ dLN. (B) Bar charts of dLN cell percentages of CD4^{+} (p=0.04) , CD4^{+}IL-2^{+} (p=0.01), and total CD4^{+}IFNγ^{+} (p=0.006) cells as well as (C) CD8^{+} (p=0.004), CD8^{+}IL-2^{+} (p=0.007) and total CD8^{+}IFNγ^{+} (p=0.03) cells. Numbers indicate % of cells within the gates, and the results shown are derived from at least two independent experiments. (D) Enhanced numbers of activated CD44^{+} tumor infiltrating CD4^{+} (p=0.009) and CD8^{+} (p=0.017) cells were detected in *Nr2f6*$^{-/-}$ (n=8) compared to *Nr2f6*$^{+/+}$ (n=8) mice, whereas no differences were observed for (E) NK (based on the marker DX5^{+}), macrophages (CD11b^{+}) or DC subsets (CD11c^{+} CD11b^{+} and CD11c^{+}CD8a^{+}). Data are shown by bar charts and error bars represent ± SEM, data were analyzed via student's t-test.

Figure S5 related to Figure 5: T cell status of healthy mice and gross examination of tumor growth in *Rag1*$^{-/-}$ mice reconstituted with either CD3$^{Nr2f6+/+}$ or CD3$^{Nr2f6-/-}$ T cells.

(A) Single cell suspension of an inguinal lymph node derived from 13-16 week old female *Nr2f6*$^{+/+}$ (n=7) or *Nr2f6*$^{-/-}$ (n=7) mice was analyzed by flow cytometry (3 independent experiments, statistics student´s t-test). (B) Gross examination of tumor growth in *Rag1*-deficient mice reconstituted with either CD3$^{Nr2f6+/+}$ or CD3$^{Nr2f6-/-}$ 14 days before subcutaneous inoculation with 1.5×10^{5} EG7 cells. Pictures of tumors were taken at the indicated time points of *Rag1*$^{-/-}$ PBS, *Rag1*$^{-/-}$CD3$^{Nr2f6+/+}$ and *Rag1*$^{-/-}$CD3$^{Nr2f6-/-}$ mice, asterisk depicts representative a picture of another *Rag1*$^{-/-}$CD3$^{Nr2f6-/-}$ mouse. (C) Flow cytometric analysis revealed increased CD4^{+} T cell numbers in the dLNs of tumor bearing *Rag*1$^{-/-}$CD3$^{Nr2f6-/-}$ mice (p=0.03) when compared to tumor dLNs of *Rag*1$^{-/-}$CD3$^{Nr2f6+/+}$ mice.

Figure S6 related to Figure 6: *Nr2f6* does neither influence nTreg & iTreg numbers and their suppressive capacity nor cell survival.

(A) Representative CFSE profiles of *Nr2f6*$^{+/+}$CD25^{-}CD4^{+} T cells either non-stimulated (-) or stimulated with anti-CD3 antibodies and mitomycin-treated APCs (+) for 3 days - without or with CD25^{high}CD4^{+} Treg cells isolated from either *Nr2f6*$^{+/+}$ or *Nr2f6*$^{-/-}$ mice at a ratio of 1:4. The frequency of divided cells is included in each histogram. (B) Proliferation of CFSE-labeled CD25^{-}CD4^{+} T cells is depicted as % of dividing cells (in bar charts). Results (mean ± SD) of two independent experiments performed in duplicates are shown. (C) Frequency of Foxp3^{+}CD25^{+} cells in peripheral LN of *Nr2f6*$^{+/+}$ or *Nr2f6*$^{-/-}$ mice was analyzed by flow cytometry. Representative dot plots (gated on CD45^{+}CD3^{+}CD4^{+}) are shown. (D) *In vitro* differentiated *Nr2f6*$^{+/+}$ or *Nr2f6*$^{-/-}$ iTreg cells (at day 5 of culture) were analyzed for their suppressive capacity using *in vitro* co-cultures. Proliferation of CFSE-labeled CD25^{-}CD4^{+} T cells (*Nr2f6*$^{+/+}$) is depicted as percent dividing cells (in bar charts) of either non-stimulated (-) or anti-CD3 antibody and mitomycin-treated APC stimulated (+) for 3 days – and in the presence of iTreg cells from either *Nr2f6*$^{+/+}$ or *Nr2f6*$^{-/-}$ mice at a ratio of 1:1. Results of 2 independent experiments each performed with T cells isolated from two individual mice (duplicates per mouse) are shown (n =4). (E) *In vitro* qRT-PCR analysis of *Foxp3* expression in CD4^{+} *Nr2f6*$^{+/+}$ cells compared to *Nr2f6*$^{-/-}$ cells during iTreg differentiation (5µg anti-CD3; 1µg anti-CD28 supplemented with 5ng/ml TGFβ and 20ng/ml IL-2) at the indicated time points (n=3). Expression was normalized to the house-keeping gene GAPDH and presented as fold induction of unstimulated control cells. Summary graphs are mean ± SD, and data are representative of at least two independent experiments, statistics were analyzed by two-way ANOVA. (F) *In vitro* differentiated iTreg cells (at day 5 of culture) were analyzed for the frequency of Foxp3^{+}CD25^{+} by flow cytometry (n=4). (G) CD4^{+} T cells were FACS-sorted from *Nr2f6*$^{+/+}$ and *Nr2f6*$^{-/-}$ spleens, RNA was isolated and RT-MLPA was performed assessing relative mRNA abundances of 42 different proteins associated with cell death (n=4, statistics: two-way ANOVA and Bonferroni post-tests). Note that gene expression with apparently different expression between genotypes was subsequently re-evaluated by qRT-PCR – no significant differences could be detected (n=4, statistics: two-way ANOVA and Bonferroni post-tests).

Figure S7 related to Figure 7: *Nr2f6* suppresses *Il2* and *Ifng* expression in CD8$^+$ T cells but not viability or apoptosis.

(A) CD8$^+$ *Nr2f6*$^{+/+}$ or *Nr2f6*$^{-/-}$ cells were activated *in vitro* with anti-CD3 (5µg) and anti-CD28 (1µg) over time (d2, d3), followed by a re-stimulation with anti-CD3 (5µg) over night (d4/re), IL-2 and IFNγ expression was analyzed via flow cytometry. Numbers within outlined areas indicate percentage of positive cells. One out of three representative experiments is shown. (B) CD8$^+$ T cells were FACS-sorted from *Nr2f6*$^{+/+}$ and *Nr2f6*$^{-/-}$ spleens, RNA was isolated and RT-MLPA was performed assessing relative mRNA abundances of 42 different proteins associated. Note that gene expression with apparently different expression between genotypes was subsequently re-evaluated by qRT-PCR – no significant differences could be detected (n=4, statistics: 2-way Anova and Bonferroni post-tests). (C) *Nr2f6*$^{+/+}$ and *Nr2f6*$^{-/-}$ CD8$^+$ T cells were activated with anti-CD3 (0.5µg or 5µg) and anti-CD28 (1µg) for 20h *in vitro*, nuclear extracts were isolated and EMSA loading amounts were controlled by performing western blots with nuclear extracts probed with lamin B. No gross differences could be observed between the genotypes using the described conditions. One out of two representative experiments is shown. (D) ChIP PCR of resting or 20h anti-CD3 (0.5µg or 5µg) and anti-CD28 (1µg) activated CD3$^+$ T cells for minimal *Il2* promoter, (E) distal (-1.4kb) *Il2* promoter or (F) minimal *Ifng* promoter, respectively. Chromatin was immunoprecipitated with anti-NR2F6, anti-NFAT2 or IgG control, and promoter sequences were quantified by real time PCR. One representative independent experiment out of two is shown.

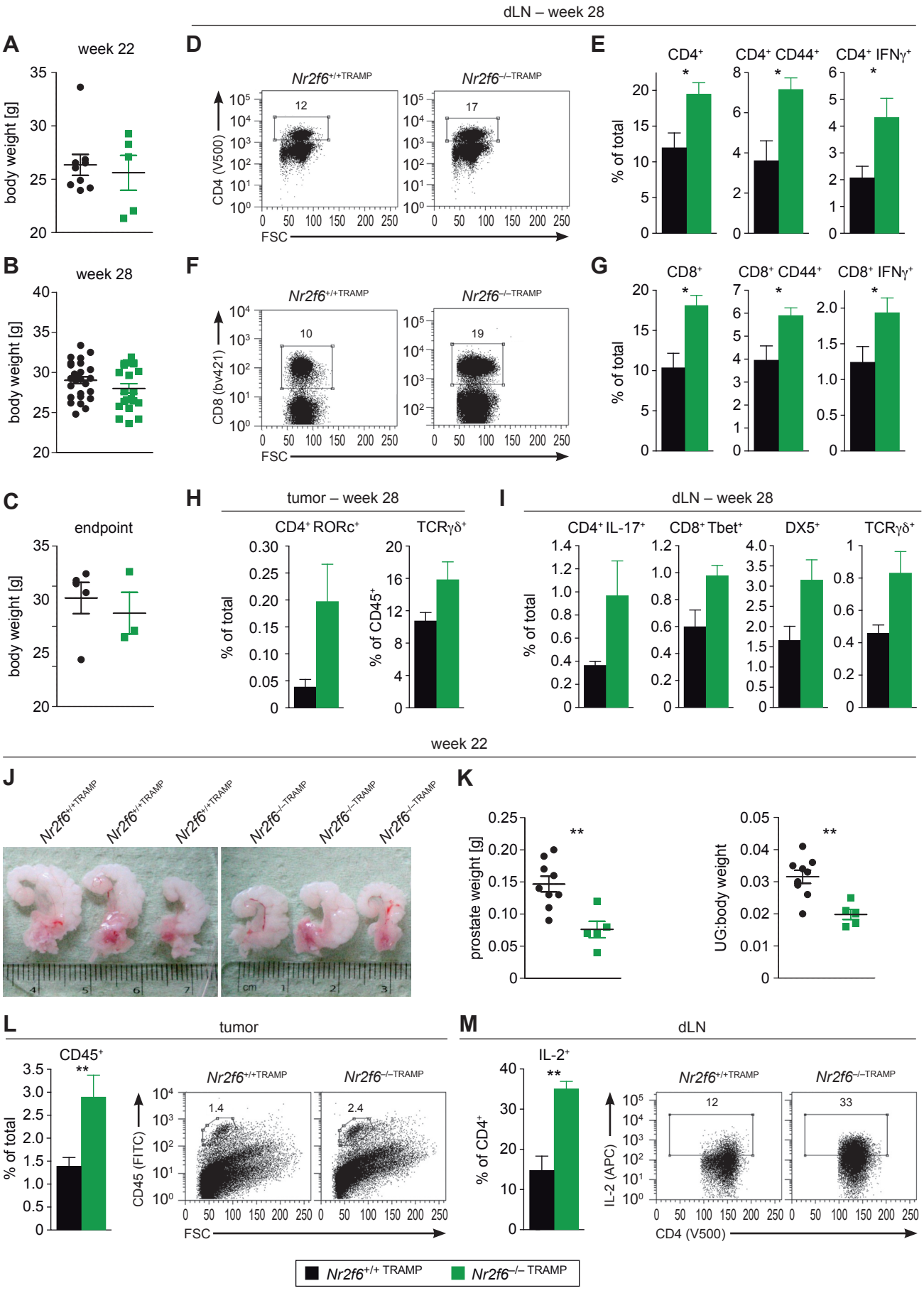
dLN – week 28
A
week 22
body weight [g]
B
week 28
C
endpoint
D
Nr2f6+/+TRAMP
Nr2f6−/−TRAMP
CD4 (V500)
FSC
E
CD4+
CD4+ CD44+
CD4+ IFNγ+
% of total
F
CD8 (bv421)
G
CD8+
CD8+ CD44+
CD8+ IFNγ+
H
tumor – week 28
CD4+ RORc+
TCRγδ+
% of CD45+
I
dLN – week 28
CD4+ IL-17+
CD8+ Tbet+
DX5+
week 22
J
K
prostate weight [g]
UG:body weight
L
tumor
CD45+
CD45 (FITC)
M
dLN
IL-2+
% of CD4+
IL-2 (APC)
Nr2f6+/+ TRAMP
Nr2f6−/− TRAMP

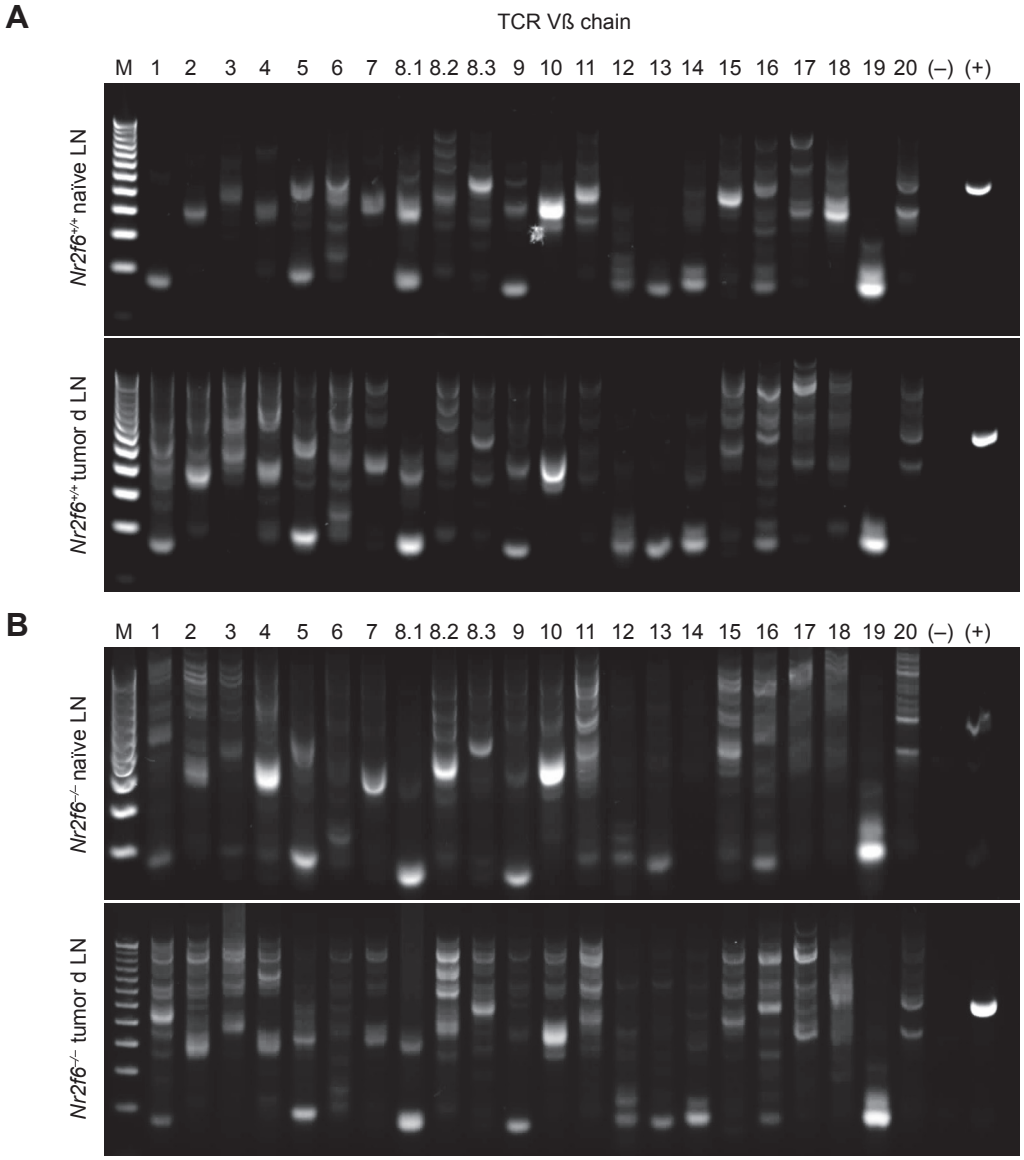
A
TCR Vß chain
M 1 2 3 4 5 6 7 8.1 8.2 8.3 9 10 11 12 13 14 15 16 17 18 19 20 (–) (+)
Nr2f6+/+ naïve LN
Nr2f6+/+ tumor d LN
B
M 1 2 3 4 5 6 7 8.1 8.2 8.3 9 10 11 12 13 14 15 16 17 18 19 20 (–) (+)
Nr2f6−/− naïve LN
Nr2f6−/− tumor d LN

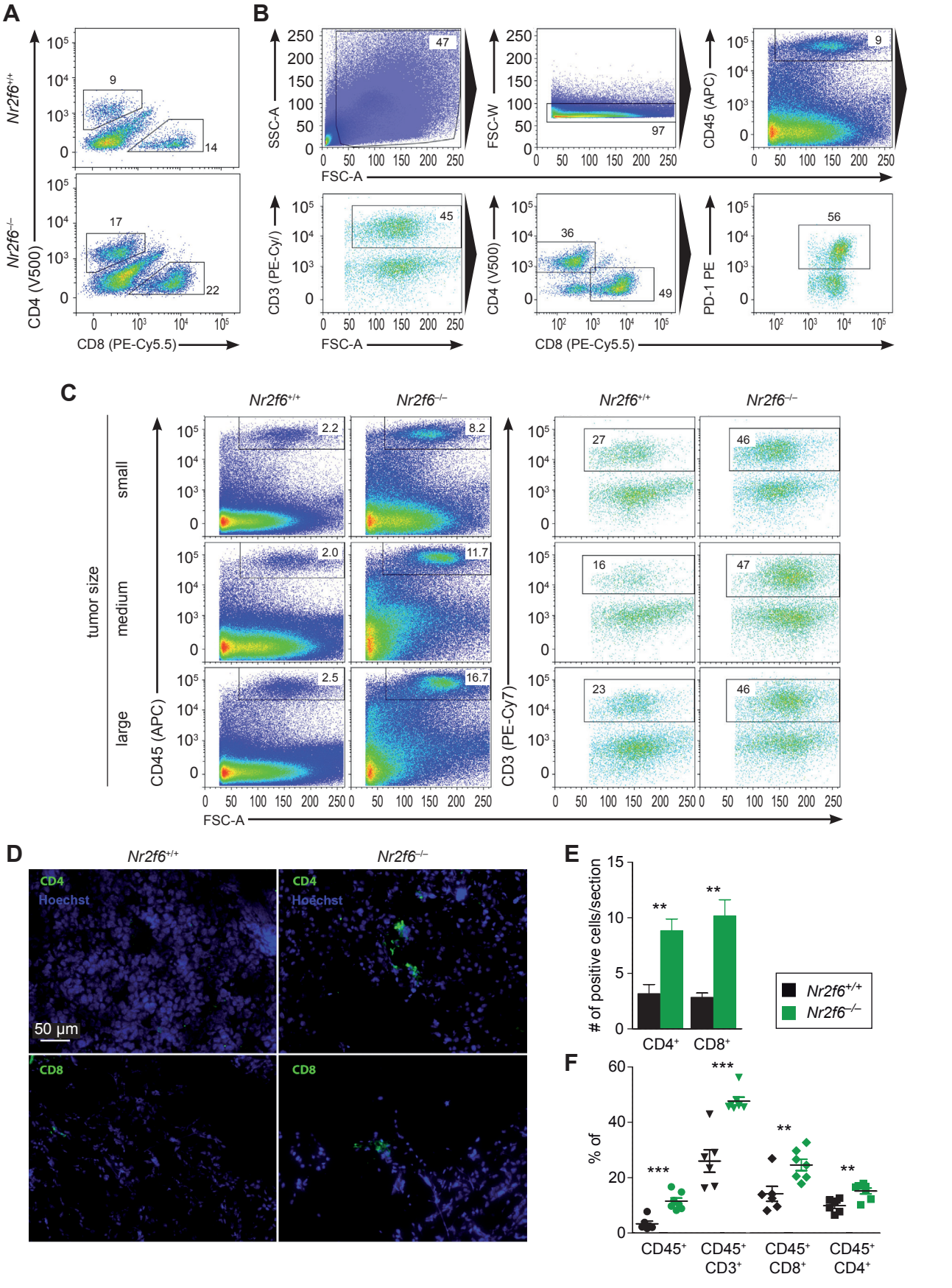
A
B
C
D
E
F
Nr2f6+/+
Nr2f6−/−
CD4 (V500)
CD8 (PE-Cy5.5)
SSC-A
FSC-A
FSC-W
CD45 (APC)
CD3 (PE-Cy/)
PD-1 PE
tumor size
small
medium
large
CD3 (PE-Cy7)
CD4
Hoechst
CD8
50 µm
# of positive cells/section
CD4+
CD8+
% of
CD45+
CD45+ CD3+
CD45+ CD8+
CD45+ CD4+

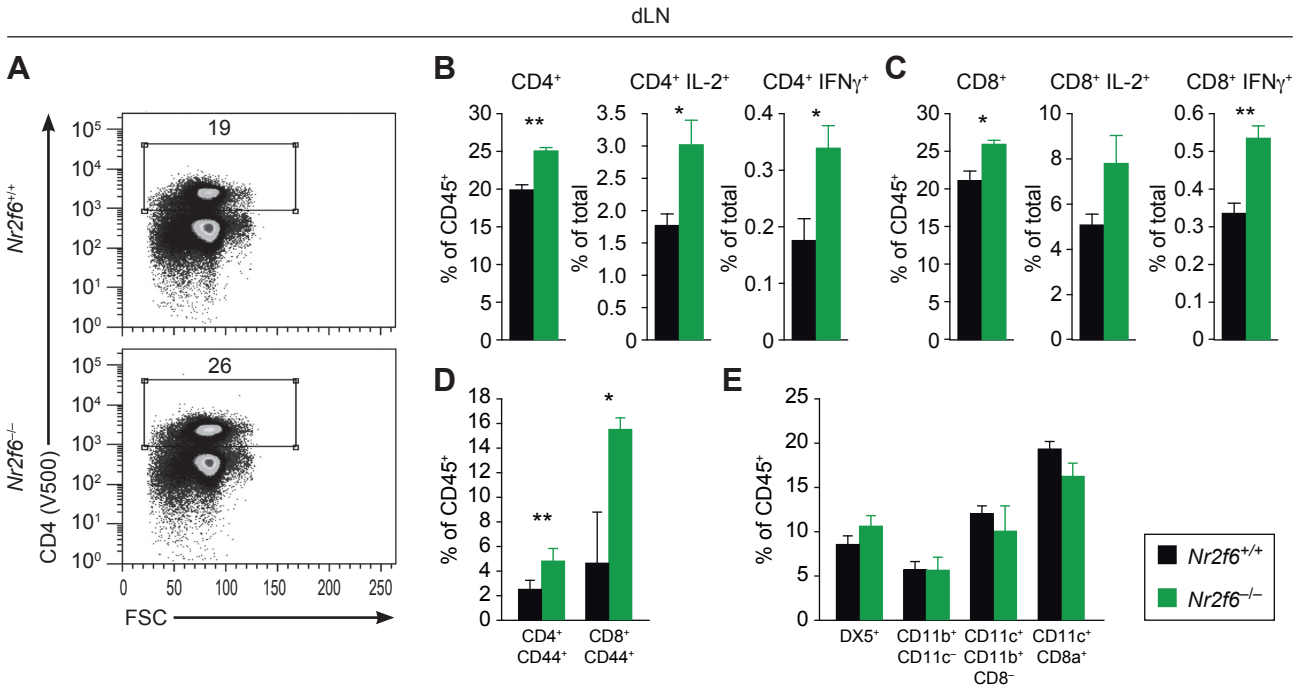
dLN
A
Nr2f6+/+
Nr2f6−/−
CD4 (V500)
FSC
19
26
B
CD4+
CD4+ IL-2+
CD4+ IFNγ+
% of CD45+
% of total
C
CD8+
CD8+ IL-2+
CD8+ IFNγ+
D
CD4+ CD44+
CD8+ CD44+
E
DX5+
CD11b+ CD11c−
CD11c+ CD11b+ CD8−
CD11c+ CD8a+
Nr2f6+/+
Nr2f6−/−

A. T cell status in healthy Nr2f6$^{+/+}$ and Nr2f6$^{-/-}$ lymph nodes (all numbers)

	***Nr2f6*$^{+/+}$**	***Nr2f6*$^{-/-}$**	p values
Total (x 10^5)	38 ± 21	35 ± 25	0.79
T cells			
CD3$^+$	18 ± 14	16 ± 11	0.85
CD3$^+$CD4$^+$	9.1 ± 7	9.4 ± 6	0.93
CD4$^+$CD25$^+$Foxp3$^+$	1.1 ± 0.8	1.1 ± 0.8	0.93
CD4$^+$CD25$^+$	6.1 ± 4.3	6.1 ± 4	0.39
CD3$^+$CD8$^+$	7.6 ± 6	6.2 ± 4.7	0.65
CD8$^+$CD25$^+$	3.2 ± 2.6	2.4 ± 2	0.56
Cytokines (4h PDBu/Ionomycin re-stimulated)			
CD4$^+$IL-2	1.6 ± 1	1.5 ± 1.2	0.91
CD4$^+$IFNγ	1.7 ± 0.7	1.7 ± 1	1.0
CD4$^+$TNFα	3.2 ± 1.9	4.1 ± 2.8	0.52
CD8$^+$IL-2	1.1 ± 0.6	0.6 ± 0.6	0.26
CD8$^+$IFNγ	1.9 ± 1.2	1.5 ± 0.9	0.53
CD8$^+$TNFα	2.5 ± 1.5	1.8 ± 1.1	0.40

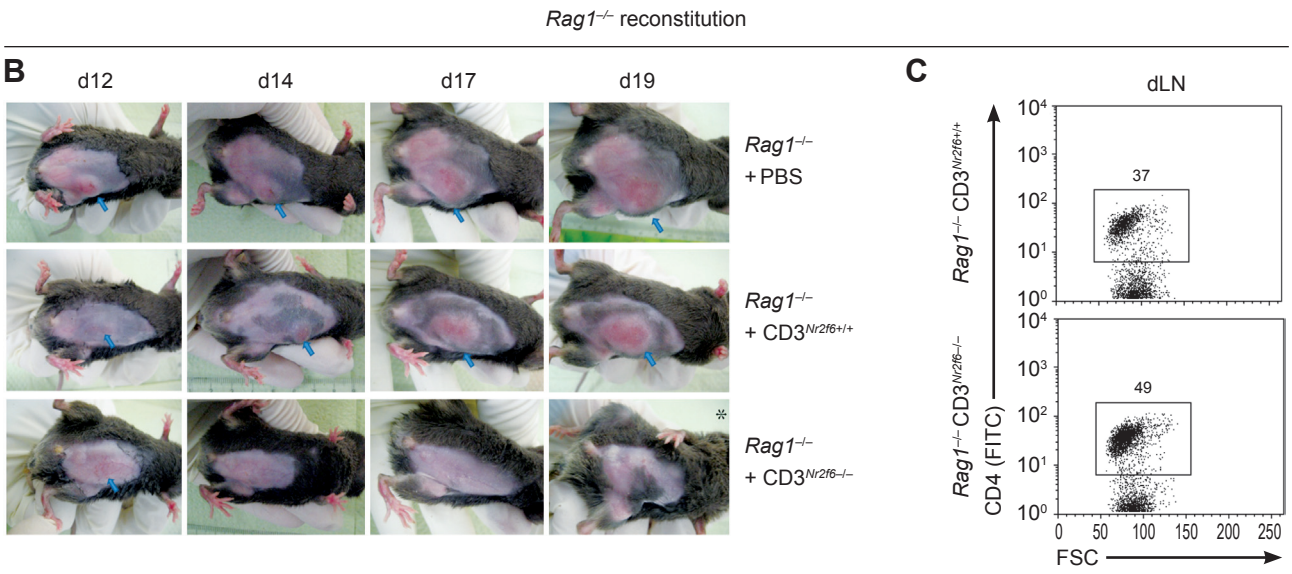

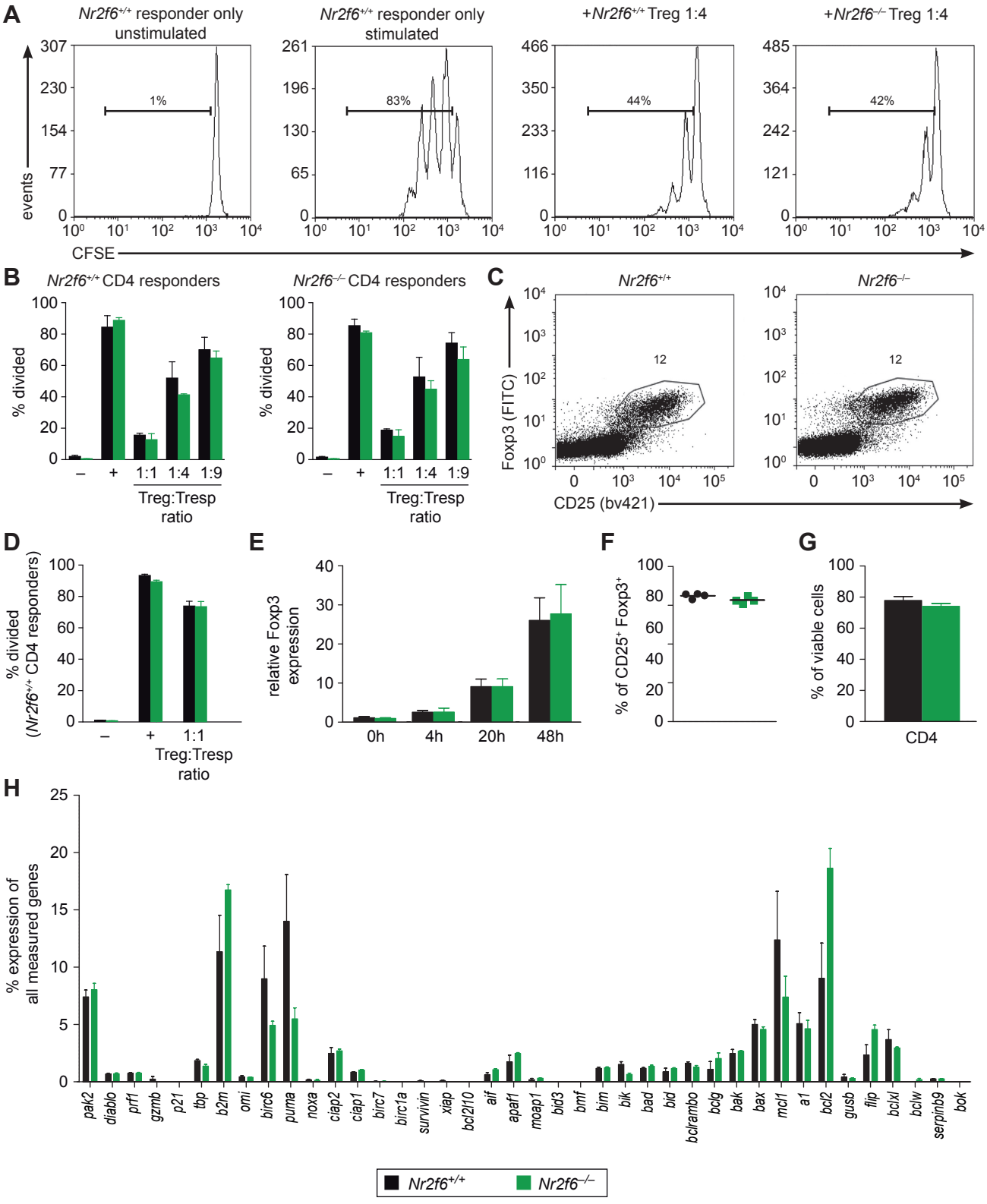
A
Nr2f6+/+ responder only unstimulated
Nr2f6+/+ responder only stimulated
+Nr2f6+/+ Treg 1:4
+Nr2f6−/− Treg 1:4
1%
83%
44%
42%
events
CFSE
B
Nr2f6+/+ CD4 responders
Nr2f6−/− CD4 responders
% divided
– + 1:1 1:4 1:9
Treg:Tresp ratio
C
Nr2f6+/+
Nr2f6−/−
12
Foxp3 (FITC)
CD25 (bv421)
D
% divided (Nr2f6+/+ CD4 responders)
– + 1:1
Treg:Tresp ratio
E
relative Foxp3 expression
0h 4h 20h 48h
F
% of CD25+ Foxp3+
G
% of viable cells
CD4
H
% expression of all measured genes
pak2 diablo prf1 gzmb p21 tbp b2m omi birc6 puma noxa ciap2 ciap1 birc7 birc1a survivin xiap bcl2l10 aif apaf1 moap1 bid3 bmf bim bik bad bid bclrambo bclg bak bax mcl1 a1 bcl2 gusb flip bclxl bclw serpinb9 bok
Nr2f6+/+
Nr2f6−/−

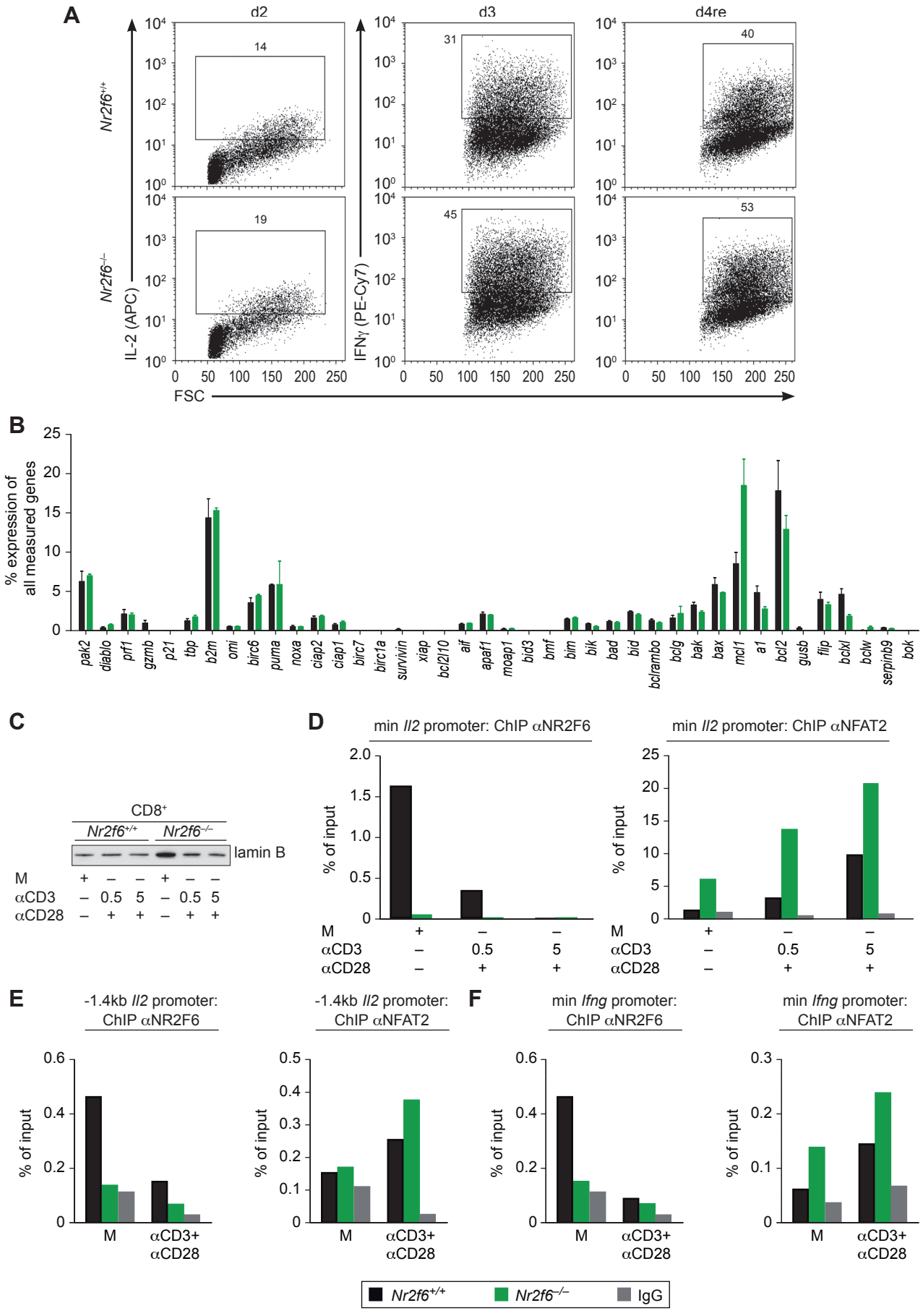
A
d2
d3
d4re
Nr2f6+/+
Nr2f6−/−
IL-2 (APC)
IFNγ (PE-Cy7)
FSC
14
19
31
45
40
53
B
% expression of all measured genes
pak2 diablo prf1 gzmb p21 tbp b2m omi birc6 puma noxa ciap2 ciap1 birc7 birc1a survivin xiap bcl2l10 aif apaf1 moap1 bid3 bmf bim bik bad bid bclrambo bclg bak bax mcl1 a1 bcl2 gusb flip bclxl bclw serpinb9 bok
C
CD8+
Nr2f6+/+
Nr2f6−/−
lamin B
M + – – + – –
αCD3 – 0.5 5 – 0.5 5
αCD28 – + + – + +
D
min Il2 promoter: ChIP αNR2F6
min Il2 promoter: ChIP αNFAT2
% of input
M + – –
αCD3 – 0.5 5
αCD28 – + +
E
-1.4kb Il2 promoter: ChIP αNR2F6
-1.4kb Il2 promoter: ChIP αNFAT2
F
min Ifng promoter: ChIP αNR2F6
min Ifng promoter: ChIP αNFAT2
M
αCD3+ αCD28
Nr2f6+/+
Nr2f6−/−
IgG